

Infrared spectroscopic investigation of erythrocyte membrane-smoke interactions due to chronic cigarette smoking

Mahmoud S. Sherif, Ali A. Mervat and Aly M. Eman

Biophysics and Laser Science Unit, Research Institute of Ophthalmology, 2 Al-Ahram Street, Giza, Egypt

Abstract. Cigarette smoking is a serious health problem throughout the world, with a complicated and not totally clear bio-effect. In this study, erythrocytes were obtained from healthy male volunteers aged 22 ± 2 years and, the possible effects of three cigarette smoking rates namely 10, 15 and 20 cigarette/day on erythrocytes membrane characteristics were examined by Fourier transform infrared spectroscopy (FTIR). The results of this study indicate many smoking-dependent variations on erythrocytes membrane without an obvious dose-response relationship. There was disruption in the acyl chain packing; changes in membrane order and phases as well as membrane proteins becoming more folded. These physico-chemical changes should have an impact on the function of erythrocytes and may explain the complex interaction of cigarette smoke mainstream with erythrocyte membrane and to some extent clarify the pathological processes associated with cigarette smoking.

Key words: Cigarette smoke — Erythrocyte membrane — FTIR — Protein — Lipid

Introduction

Cigarette smoking – a worldwide social habit – is associated with well documented numerous health hazards that include lung cancer, stroke, respiratory, cardiovascular diseases and osteoporosis (Mello 2010). These health risks result from the entrance of the mainstream smoke into the blood which leads to alterations in the blood constituents, plasma, erythrocytes, platelets and leukocytes (Freeman et al. 2005), and have been attributed to the abundance of reactive oxygen species and reactive nitrogen species (Barua et al. 2003). More smoking health hazards that should be addressed are the ocular ones aggravated by cigarette smoke which include dry eye (Arffa 1991), conjunctival irritation, age-related macular degeneration, cataract, ocular inflammation and change in tear characteristics (Satici et al. 2003; Sprague et al. 2006; Thorne et al. 2008; Lin et al. 2010; Roesel et al. 2011). In addition, the retina is known to have the highest rate of oxygen consumption of any organ in the body (Kewal 2011). Therefore any alterations in the structure and/or function of the erythrocyte membranes should have an impact on retinal function.

Padmavathi et al. (2010) found that chronic cigarette smoking alters the content of individual phospholipids of erythrocytes membrane that was associated with increased membrane lipid peroxidation. The erythrocytes membrane-cigarette smoke interactions appear to be more complex and the exact mechanism that enhance these effects remain uncertain. Therefore, the present study is aimed to understand the effect of chronic cigarette smoke exposure on the erythrocyte membrane structural and conformational characteristics that were studied by Fourier transform infrared spectroscopy (FTIR) while taking into account the smoking rate (number of cigarette smoked/day) and the dose-response relationship if any.

Participants and Methods

Subjects

Four groups of healthy male subjects were involved in this study, where each group composed of 25 age-matched subjects (22 ± 2 years). Three groups were cigarette smokers for 3 ± 1 year but differ in the daily smoking rate as 10, 15 and 20 cigarette/day (cig/day), and the last group served as the control one. All study subjects had normal renal and hepatic functions with no evidence of any acute infection

Correspondence to: Sherif Siddick Mamhmoud, Biophysics and Laser Science Unit, Research Institute of Ophthalmology, P.O. Box 90, 2 Al-Ahram Street, Giza, Egypt
E-mail: sheri_sm@yahoo.com

or active inflammatory process. None of the subjects had hypertension, were taking any medications or receiving vitamin supplementation. There was no significant obesity observed between all subjects ($BMI = 22.4 \pm 3.6$), as well as cholesterol (155 ± 15 mg/dl) and triglycerides (125 ± 8 mg/dl), with normal fasting blood glycemic level (90 ± 5 mg/dl). All subjects signed an informed consent with tenets of the Declaration of Helsinki.

Preparation of erythrocyte membranes

Blood was obtained by veinpuncture, collected into heparinized syringes and immediately centrifuged at $500 \times g$ at $4^\circ C$ for 10 min. The plasma and buffy coat were discarded, and erythrocytes were re-suspended and washed three times in physiological saline (0.9% NaCl). Erythrocyte membranes were prepared as previously mentioned by Sprague et al. 2006. The washed erythrocytes were added to 200 ml of hypotonic buffer (5 mmol/l Tris-HCl, 2 mmol/EDTA, pH 7.4) and stirred vigorously for 20 min. The mixture was centrifuged at $23,000 \times g$ for 15 min, and the supernatant was discarded. After repeating the last step one more time, membranes were pooled, resuspended in buffer and centrifuged. Finally, after discarding the supernatant, membranes were freeze-dried and kept under N_2 gas atmosphere for further analysis.

Fourier transform infrared spectroscopy

Erythrocytes membrane was mixed with finely ground powder KBr to prepare the KBr-disks that were used in analysis. This mixture was placed in a special holder pro-

vided by the manufacturer and pressed under vacuum at 3 tons (13.8 MPa) for 2 min to produce IR-KBr disks (Sherif 2010). FTIR measurements were carried out using Nicolet-iS5 infrared spectrometer (ThermoFisher Scientific Inc, Madison, USA) with effective resolution of 2 cm^{-1} . Each spectrum was derived from 100 sample interferograms. The spectrometer was operated under a continuous dry N_2 gas purge to remove interference from atmospheric CO_2 and H_2O vapor. The spectra were baseline corrected and then smoothed with Savitsky–Golay to remove the noise before Fourier transformation. Three spectra from each sample were obtained and averaged using OriginPro 7.5 software to obtain the final average group spectrum that was normalized and analyzed for the following spectral regions: $4000\text{--}3000\text{ cm}^{-1}$ (NH-OH region), $3000\text{--}2800\text{ cm}^{-1}$ (CH stretching region), $1800\text{--}1600\text{ cm}^{-1}$ (amide I region) and $1600\text{--}900\text{ cm}^{-1}$ (fingerprint region), and then subjected to curve enhancement analysis using a combination of Fourier deconvolution and non-linear curve fitting. The second derivative of the group spectrum was employed to confirm the number of the estimated peaks.

Statistical analysis

Results were calculated and expressed as mean \pm standard deviation (SD). Comparison between multiple groups was performed using analysis of variance (ANOVA); commercially available statistical software package (SPSS-11 for Windows) was used where the significance level was set at $p < 0.05$. All spectral analyses were performed with OriginPro 7.5 software package (Origin Lab Corporation, Northampton, MA, USA).

Results

The erythrocytes infrared spectra were analyzed according to the following described regions.

NH-OH region

In Figure 1, the contour of the control erythrocytes membrane indicates the presence of several absorption bands that were resolved into 8 structural components using the curve enhancement procedure as given in Table 1. In the same context, the contour of smokers' erythrocytes membrane was also resolved into 8 structural peaks that differed in band position, band area and bandwidth as well as their assignment Table 1. The stretching OH ($_{str}OH$) compositional bands were reduced from four components in the control and 10 cig/day groups to three structural components as the number of smoked cigarettes increased to 15/20 daily.

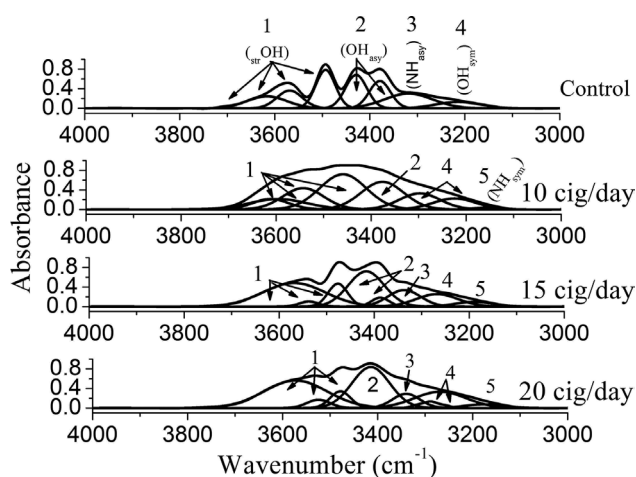


Figure 1. Erythrocytes membrane NH-OH region ($4000\text{--}3000\text{ cm}^{-1}$) of the control group and cigarette smoking ones, showing the underlying bands that detected upon using curve fitting analysis. The numbers above the peaks to facilitate their assignment.

The two structural components of the asymmetric OH ($_{\text{asym}}\text{OH}$) bond were reduced to one component in two groups only; 10 cig/day and 20 cig/day that were characterized by significantly increased bandwidth and band area. At a smoking rate of 15 cig/day, the two detected structural component show paradox characteristics; where the higher frequency band has an increased band area and bandwidth while the lower frequency one has decreased band area and bandwidth. On the other hand, symmetric OH ($_{\text{sym}}\text{OH}$) band showed a different behavior; increased vibrational frequency and band area that were associated to different smoking rates, this is in addition to its splitting into 2 structural components at a daily smoking rate of 10 and 20 cigarette compared to control one as shown in Table 1.

For all smoking groups, the symmetric NH ($_{\text{sym}}\text{NH}$) stretching vibrational mode was detected. Comparing the three smoking groups, it is noticed that this vibrational mode was characterized by increased vibrational frequency, band area as well as bandwidth as the number of cigarette smoked increased from 10 to 15/20 daily while, the asymmetric vibrational mode of the NH band ($_{\text{asym}}\text{NH}$) was restricted at 10 cig/day smoking group, then detected again as the smoking rate increased to 15/20 daily and is characterized by increased vibrational frequency and bandwidth as well. The band area was reduced at 20 cig/day smoking group.

CH stretching region

The CH stretching pattern of the control erythrocytes indicated the presence of four absorption bands that were centered at 2962 ± 3 , 2920 ± 2 , 2870 ± 2 and $2846 \pm 3 \text{ cm}^{-1}$ and assigned to asymmetric CH_3 ($_{\text{asym}}\text{CH}_3$), asymmetric CH_2 ($_{\text{asym}}\text{CH}_2$), symmetric CH_3 ($_{\text{sym}}\text{CH}_3$) and symmetric CH_2 ($_{\text{sym}}\text{CH}_2$) respectively (Figure 2). This pattern was changed in all smoking subjects. The number of absorption bands was decreased at 10 and 15 cig/day smoking groups with restricted $_{\text{sym}}\text{CH}_2$ vibrational mode. Subjects with smoking rate of 20 cig/day showed a different CH vibrational pattern; in addition to the restricted $_{\text{sym}}\text{CH}_2$ mode, there is an additional stretching mode of vibration that was detected at $2904 \pm 2 \text{ cm}^{-1}$ and attributed to aliphatic CH (CH_{aliph}). There is no change in band position or bandwidth of smoking subjects' $_{\text{asym}}\text{CH}_3$ or $_{\text{sym}}\text{CH}_3$ while, the band position of smoking $_{\text{asym}}\text{CH}_2$ was found to be increased relative to the control pattern as given in Table 2. This table also shows undetectable changes in band area of $_{\text{asym}}\text{CH}_3$, $_{\text{asym}}\text{CH}_2$ and $_{\text{sym}}\text{CH}_3$ bands relative to their corresponding control ones.

Amide I region

Analysis of amide I band by using the curve enhancement procedure (Figure 3) resolved the control band into three

Table 1. Vibrational frequencies, band area and bandwidth of NH-OH structural components of control erythrocytes membrane and cigarette smoking groups

Group	strOH	$_{\text{asym}}\text{OH}$		$_{\text{sym}}\text{OH}$		$_{\text{asym}}\text{NH}$		$_{\text{sym}}\text{NH}$			
Control	3702 ± 2	3616 ± 2	3569 ± 4	3493 ± 4	3429 ± 2	3379 ± 3	3319 ± 2	-	3214 ± 4	-	-
	0.7 ± 0.2	29 ± 5	24 ± 4	40 ± 2	39 ± 5	31 ± 2	38 ± 4	-	15 ± 3	-	-
10 cig/day	29 ± 4	81 ± 9	50 ± 2	36 ± 3	41 ± 3	40 ± 3	100 ± 8	-	92 ± 5	-	-
	-	3613 ± 3	3595 ± 3 [†]	3543 ± 3	3459 ± 3 [†]	3377 ± 4	-	3298 ± 3 [†]	-	3224 ± 3 [†]	3156 ± 3
15 cig/day	-	32 ± 3	20 ± 4	47 ± 8	88 ± 8 [†]	63 ± 7 [†]	-	35 ± 6 [†]	-	28 ± 3 [†]	3 ± 1
	-	73 ± 5	118 ± 13 [†]	84 ± 6	96 ± 10 [†]	88 ± 9 [†]	-	84 ± 6	-	87 ± 10	53 ± 10
20 cig/day	-	-	3569 ± 2	3538 ± 2	3476 ± 2 [†]	3417 ± 4 [†]	3385 ± 4	3337 ± 3 [†]	3267 ± 3 [†]	-	3182 ± 4
	-	-	79 ± 8 [†]	8 ± 2	24 ± 3 [†]	68 ± 3 [†]	9 ± 3 [†]	29 ± 8	28 ± 5 [†]	-	12 ± 4
20 cig/day	-	-	129 ± 3 [†]	35 ± 2	36 ± 3	73 ± 5 [†]	32 ± 2 [†]	66 ± 9 [†]	85 ± 4	-	77 ± 5
	-	-	3573 ± 3 [†]	3524 ± 1	3478 ± 3 [†]	3414 ± 2 [†]	-	3340 ± 3 [†]	3292 ± 2 [†]	3268 ± 4 [†]	3179 ± 4
20 cig/day	-	-	93 ± 8 [†]	10 ± 3	15 ± 2 [†]	83 ± 5 [†]	-	21 ± 5 [†]	5 ± 2 [†]	45 ± 7 [†]	8 ± 1
	-	-	131 ± 7 [†]	44 ± 2	38 ± 7	77 ± 3 [†]	-	54 ± 6 [†]	35 ± 7 [†]	105 ± 9	78 ± 3

First line in each cell indicates the wavenumber in cm^{-1} , second line reflects the band area and the third line indicates the bandwidth in cm^{-1} . † Statistically significant vs. control.

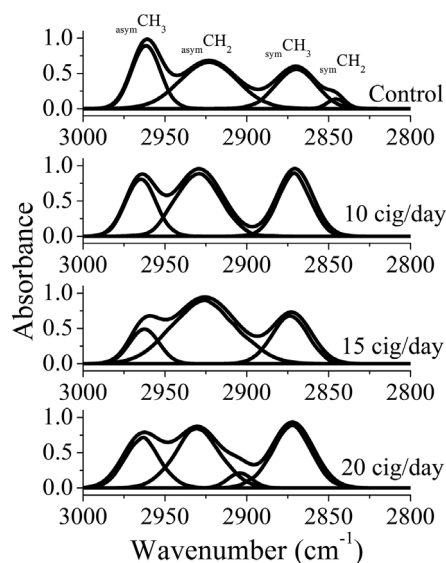


Figure 2. Stretching CH region ($3000\text{--}2800\text{ cm}^{-1}$) of control and cigarette smoking erythrocytes membrane.

structural components that are centered at 1688 ± 3 , 1655 ± 2 and $1623 \pm 2\text{ cm}^{-1}$ and can be attributed to β -turn structure, α -helix and β -sheet, respectively (Lin et al. 1998). Due to cigarette smoking, the contour of amide I can be resolved into five structural components with additional structural components that were centered on 1663 ± 3 and $1612 \pm 2\text{ cm}^{-1}$ and can be assigned to turns and antiparallel β -sheet. The significance of these results is presented in Table 3, which shows the area percentage of each structural component relative to the total band area. Alpha-helix content is sig-

Table 2. Erythrocytes membrane characteristics of CH stretching region of control and cigarette smoking groups

Group	asymCH ₃	asymCH ₂	CH _{aliph}	symCH ₃	symCH ₂
	2962 ± 3	2920 ± 2	–	2870 ± 2	2846 ± 3
Control	20 ± 2	31 ± 4	–	23 ± 3	1.8 ± 0.2
	17 ± 3	35 ± 5	–	25 ± 3	10 ± 2
	2965 ± 2	2929 ± 3	–	2871 ± 2	–
10 cig/day	20 ± 2	35 ± 5	–	26 ± 3	–
	18 ± 4	29 ± 4	–	22 ± 4	–
	2963 ± 3	2926 ± 3 [†]	–	2872 ± 2	–
15 cig/day	18 ± 5	42 ± 9	–	21 ± 4	–
	18 ± 4	39 ± 4	–	24 ± 3	–
	2964 ± 2	2930 ± 3 [†]	2904 ± 2	2872 ± 2	–
20 cig/day	21 ± 4	31 ± 3	4 ± 1	30 ± 6	–
	23 ± 5	28 ± 5	14 ± 3	26 ± 3	–

First line in each cell represents the frequency in cm^{-1} , second line indicates the band area and third line reflects the bandwidth in cm^{-1} . [†] statistically significant vs. control.

Table 3. Protein secondary structure components expressed as the area percentage of each structural component relative to the total band area

Group	α -helix	β -turns	β -sheet	Turns
Control	80 ± 4.8	10.4 ± 1.1	9.6 ± 2.8	–
10 cig/day	54.1 ± 3.1 [†]	14.8 ± 1.7 [†]	17.3 ± 1.6 [†]	13.8 ± 3.3
15 cig/day	32.2 ± 2.4 [†]	23.7 ± 2.7 [†]	19.2 ± 2.5 [†]	24.9 ± 2.6
20 cig/day	37.9 ± 2.3 [†]	20.9 ± 1.8 [†]	20.8 ± 1.3 [†]	20.4 ± 4.2

[†] statistically significant vs. control.

nificantly decreased in all smoking groups concomitant with a significant increase in β -turn and β -sheet structures. The interesting finding is the detection of Turns-structure that was associated to all smoking rates (Rose et al. 1985).

Fingerprint region

The other frequency range under consideration is $1600\text{--}900\text{ cm}^{-1}$, which is shown in Figure 4. There is broadening in the contour of smoking groups with reduction in the absorption intensities; concomitant to reduced number of the estimated peaks. The control pattern shows seven absorption bands with eleven estimated structural peaks as given in Table 4. No change in the band characteristics (frequency, bandwidth or band area) of amide II while, reduced band area of asymmetric COOC (asymCOOC) band was found. The splitting noticed in both scissoring CH_2 (scissCH_2) and symmetric PO_2 (symPO_2) bands of control group was restricted in all smoking ones. Another

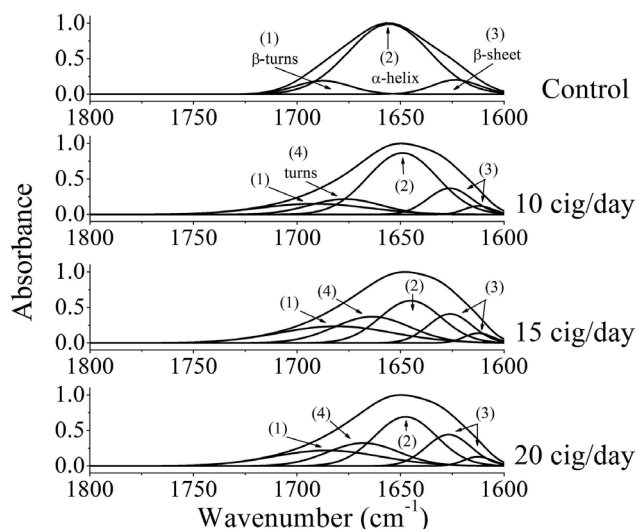


Figure 3. Analysis of Amide I band showing the mean peak and the underlying structural components. The numbers above the peaks is to facilitate their assignment.

common feature noticed in these two bands is the increased bandwidth that was associated to different smoking rates. The band position of $_{\text{sym}}\text{PO}_2$ was sensitive to all smoking rates (decreased), while that of $_{\text{sciss}}\text{CH}_2$ was increased in 10 and 15 cig/day groups only. The symmetric COO ($_{\text{sym}}\text{COO}$) higher frequency estimated component was characterized by decreased vibrational frequency in all smoking subjects, and this is contrary to the lower frequency one where its vibrational frequency was increased while, both of them were associated with reduced band area and vibrational motion (bandwidth). Reduced band position and band area was detected for the asymmetric PO_2 ($_{\text{asym}}\text{PO}_2$) band without any change in its vibrational motion. Also, no splitting was found in the rocking CH_3 ($_{\text{rock}}\text{CH}_3$) band in all smoking groups with fluctuations in its vibrational frequency that was associated with increasing vibrational motion. In the same context, increased band area was also detected for the higher frequency band relative to its corresponding control band.

Discussion

Cigarette mainstream is a complex and heterogeneous mixture that contains volatile chemicals (e.g. formaldehyde), particles (e.g. nicotine) and gases (e.g. carbon monoxide). Moreover, a puff of cigarette smoke can contain about 300 million to 3.5 billion particles (Satici et al. 2003; Galor and Lee 2011). It also contains more than 10^{14} low-molecular carbon and oxygen centered radicals *per* puff with almost 500 ppm nitric oxide and other reactive nitrogen oxides (Pryor et al. 1993).

The obtained results from NH-OH region showed several fluctuated changes associated to different smoking rates, and only two structural components – namely $_{\text{str}}\text{OH}$ that detected at an average vibrational frequency of $3535 \pm 10 \text{ cm}^{-1}$ and $_{\text{sym}}\text{NH}$ one – can be directly related to cigarette smoking, meaning that can be used to monitor/probe the impact of cigarette smoking on the erythrocytes membrane. This region also indicates that the detected $_{\text{sym}}\text{NH}$ mode should had another impact on the function of erythrocytes membranes since it is an indicator that the membrane become more ordered as previously reported by Schultz et al. (1998) that symmetric stretching vibrations are functioning as a marker for membrane order. In spectroscopy, the area under the peak is used as an estimate of the concentration of the compound. Regarding this issue, the increased membrane order is also evident by the increased concentration of all structural components of $_{\text{sym}}\text{OH}$ band and to clarify this last finding, the ratio of total band areas of $_{\text{sym}}\text{OH}/_{\text{asym}}\text{OH}$ in control erythrocytes was 0.2 while it increased as the smoking rate increased to 15 and 20 cigarette/day to be 0.4 and 0.6 respectively. In the same context, the relative-total concentration of the individual structural

Table 4. Analysis of erythrocytes membrane fingerprint region of all subjects included in the study

Group	Amide II	$_{\text{sciss}}\text{CH}_2$	$_{\text{sym}}\text{COO}$	$_{\text{rock}}\text{CH}_3$	$_{\text{asym}}\text{PO}_2$	$_{\text{asym}}\text{COOC}$	$_{\text{sym}}\text{PO}_2$
Control	1548 ± 2	1483 ± 3	1408 ± 2	1327 ± 1	1254 ± 4	1166 ± 1	1114 ± 2
	35.1 ± 3	12.4 ± 2	12 ± 1	2 ± 0.7	18 ± 4	5 ± 0.4	5 ± 2
	30 ± 3	25 ± 1	26 ± 3	11 ± 2	61 ± 8	26 ± 4	30 ± 3
10 cig/day	1546 ± 1	1694 ± 2 [†]	1392 ± 2 [†]	–	1240 ± 2 [†]	1165 ± 2	1089 ± 3 [†]
	37 ± 2	13 ± 3	4.4 ± 0.6 [†]	–	6.3 ± 1 [†]	2.9 ± 0.8 [†]	4.2 ± 0.5
	32 ± 1	85 ± 12 [†]	14 ± 4 [†]	–	57 ± 5	36 ± 9	45 ± 2 [†]
15 cig/day	1550 ± 3	1515 ± 1 [†]	1395 ± 1 [†]	1324 ± 2	1242 ± 3 [†]	1168 ± 3	1089 ± 3 [†]
	40 ± 5	12 ± 3	3.4 ± 0.4 [†]	14 ± 4 [†]	6 ± 2 [†]	1.3 ± 0.8 [†]	14 ± 2 [†]
	33 ± 2	61 ± 9 [†]	13 ± 2 [†]	66 ± 12 [†]	65 ± 7	22 ± 5	98 ± 10 [†]
20 cig/day	1548 ± 2	1484 ± 3	1398 ± 2 [†]	1317 ± 2 [†]	1243 ± 2 [†]	1168 ± 3	1096 ± 3 [†]
	37 ± 2	16 ± 2	1.3 ± 0.4 [†]	21 ± 6 [†]	6 ± 0.6 [†]	2.1 ± 0.6 [†]	6 ± 0.6
	31 ± 2	90 ± 12 [†]	12 ± 3 [†]	77 ± 10 [†]	60 ± 4	29 ± 3	60 ± 7 [†]

First line in each cell represents the frequency in cm^{-1} , the second line indicates the band area while the last line indicates the bandwidth in cm^{-1} . [†] statistically significant vs. control.

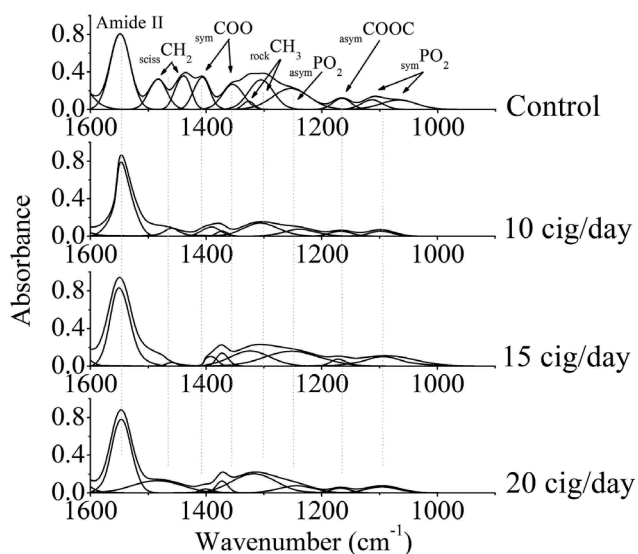


Figure 4. FTIR spectra of fingerprint region of different erythrocytes membranes involved in this study.

components of str-OH bands was also found to be increased from 93 ± 4 in the control erythrocytes and reaches 187 ± 5 , 111 ± 2 and 118 ± 2 that corresponds to smoking rates of 10, 15 and 20 cigarette/day. The OH bond can be found in many membrane constituents and one of these possibilities is cholesterol, which may support this finding about increased erythrocytes membrane order.

On the other hand, the CH region was greatly affected by all smoking rates involved in this study and, in particular symmetric and asymmetric CH_2 bands which again give the impetus about the possibility of using these two bands to probe cigarette smoking-induced changes. This vibrational region is used generally to characterize the lipid molecules within the cell membrane. As shown in Figure 2 and Table 2, there are changes in the molecular environment of the asym-CH_2 as reflected by increased band position. The disappeared sym-CH_2 mode of vibration was previously reported by Szalontai et al. (2003) and Sherif (2010) and referred to it as a lipid-related phenomenon correlated with changes in protein secondary structure. This vibrational region can also be used to monitor the compositional changes of the erythrocytes membrane by considering the concentration ratio asym-CH_3 (lipids)/ sym-CH_3 (protein). For control erythrocyte membrane this ratio was found to be 0.9, while it decreased for smoking rates of 10 and 20 cigarette/day to 0.8 and 0.7, respectively; and mimicking the control value for 15 cigarette/day group. This reveals that erythrocyte membranes, and due to different smoking rates, are suffer from fluctuating lipid/protein ratio and it may be a buffering response for the induced cigarette stress.

Proteins in biological membranes can perturb the lipid environment and, depending on their nature and concentration, influence membrane fluidity (Chapman et al. 1979; Szalontai et al. 2003). The erythrocyte proteins are essential for the linkage connecting the membrane skeleton to the lipid bilayer, which is also essential for membrane stability (Lux et al. 1978). The skeletal protein network appears to play a key role in the maintenance of the membrane's discoid shape and in restriction of the lateral mobility of its molecules (Goodman and Branton 1978; Low et al. 1991). Amide I mode of vibration in the $1800\text{--}1600\text{ cm}^{-1}$ spectral region was used to study the protein secondary structure in infrared spectroscopy since this absorption is mainly associated with C=O stretching vibrations and it is suitable as a probe to determine the different secondary structures and polypeptides (Susi et al. 1967; Lux 1979). The obtained results (Figure 3 and Table 3) show that the protein secondary structure was affected by all smoking rates. It has been suggested that protein insolubility is functioning in the content of β -sheet structure: more β -sheet structure means more insoluble protein and, the formation of β -sheet can be deduced by firstly increasing the disordered structure of the helical structure, and then, the disordered chains aggregate to form β -sheet structure (Zagorski and Barrow 1992; Lin et al. 1998). Accordingly, smoking rates of 10, 15 and 20 cig/day strongly affect the solubility of erythrocytes membrane protein and resulted in insoluble protein as indicated by both reduced α -helix content and the associated increased β -sheet content, as well as protein becomes more folded due to increased β -turns and turns structure. These complex changes in erythrocytes membrane protein secondary structure explain the disappearance of sym-CH_2 mode of vibrations as previously mentioned. Maintenance of appropriate membrane lipid composition and fluidity are important for the proper functioning of integral membrane proteins, membrane bound enzymes, receptors and ion channels (Swapna et al. 2006; Reddy et al. 2009).

The complicated effects of smoking are also evident in the fingerprint region. The erythrocytes membrane pattern shown in Figure 4 and analyzed in Table 4, reflect the fact that erythrocytes hydrocarbon chains (sciss-CH_2 and rock-CH_3) and the phospholipids (sym-PO_2) can be found in two different phases, which greatly affected – by all smoking rates involved in this study – and turned into one phase. Moreover, the sciss-CH_2 vibrations are characteristic of the nature of the acyl chain packing (Cameron et al. 1980; Swapna et al. 2006) hence; cigarette smoking has an effective impact on the acyl chain packing within the erythrocytes membrane.

Altogether showed that erythrocytes membrane reacts positively with cigarette smoke mainstream in a complicated manner without any specific trends where all membrane constituents are involved, and there were certain vibrational modes that can be used as a probing marker for cigarette

smoking aggravated changes. Regardless the number of cigarette smoked/day, it affects the NH-OH region of either proteins or phospholipids where each smoking rate has its own effects. Cigarette smoking resulted in increased erythrocytes membrane order which affects the membrane fluidity and accordingly its function. The changes in protein secondary structure, acyl chain packing and the detected compositional changes of the CH region could influence the discoid shape of the erythrocytes.

Conflict of interest. There are no conflicts of interest related to any of the participants in this research work.

References

- Arffa R. C. (1991): Grayson's Diseases of the Cornea. St Louis, Mosby Year Book
- Barua R. S., Ambrose J. A., Srivastava S., DeVoe M. C., Eales-Reynolds L. J. (2003): Reactive oxygen species are involved in smoking induced dysfunction of nitric oxide biosynthesis and upregulation of endothelial nitric oxide synthase: an in vitro demonstration in human coronary artery endothelial cells. *Circulation* **107**, 2342–2347
<https://doi.org/10.1161/01.CIR.0000066691.52789.BE>
- Cameron D. G., Casal H. L., Mantsch H. H. (1980): Characterization of the pretransition in 1,2-dipalmitoyl-sn-glycero-3-phosphocholine by Fourier transform infrared spectroscopy. *Biochemistry* **19**, 3665–3672
<https://doi.org/10.1021/bi00557a005>
- Chapman D., Gomez-Fernandez J. C., Goni F. M. (1979): Intrinsic protein-lipid interactions. Physical biochemical evidence. *FEBS Lett.* **98**, 211–223
[https://doi.org/10.1016/0014-5793\(79\)80186-6](https://doi.org/10.1016/0014-5793(79)80186-6)
- Freeman T. L., Haver A., Duryee M. J., Tuma D. J., Klassen L. W., Hamel F. G., White R. L., Rennard S. I., Thiele G. M. (2005): Aldehydes in cigarette smoke react with the lipid peroxidation product malonaldehyde to form fluorescent protein adducts on lysines. *Chem. Res. Toxicol.* **18**, 817–824
<https://doi.org/10.1021/tx0500676>
- Galor A., Lee D. J. (2011): Effects of smoking on ocular health. *Curr. Opin. Ophthalmol.* **22**, 477–482
<https://doi.org/10.1097/ICU.0b013e32834bbe7a>
- Goodman S. R., Branton D. (1978): Spectrin binding and the control of membrane protein mobility. *J. Supramol. Struct.* **8**, 455–463
<https://doi.org/10.1002/jss.400080408>
- Kewal K. J. (2011): *The Handbook of Neuroprotection*. Humana Press, Springer
- Lin P., Loh A. R., Margolis T. P., Acharya N. R. (2010): Cigarette smoking as a risk factor for uveitis. *Ophthalmology* **117**, 585–590
<https://doi.org/10.1016/j.ophtha.2009.08.011>
- Lin S. Y., Li M. J., Liang R. C., Lee S. M. (1998): Non-destructive analysis of the conformational changes in human lens lipid and protein structures of the immature cataracts associated with glaucoma. *Spectrochim. Acta A Mol. Biomol. Spectrosc.* **54**, 1509–1517
[https://doi.org/10.1016/S1386-1425\(98\)00175-9](https://doi.org/10.1016/S1386-1425(98)00175-9)
- Low P. S., Willardson B. M., Mohandas N., Rossi M., Shohet S. (1991): Contribution of the band 3-ankyrin interaction to erythrocyte membrane mechanical stability. *Blood* **77**, 1581–1586
- Lux S. E. (1979): Spectrin-actin membrane skeleton of normal and abnormal blood cells. *Semin. Hematol.* **16**, 21–51
- Lux S. E., John K. M., Ukena T. E. (1978): Diminished spectrin extraction from ATP depleted human erythrocytes. Evidences relating spectrin to changes in erythrocyte shape and deformability. *J. Clin. Invest.* **61**, 815–827
<https://doi.org/10.1172/JCI108996>
- Mello N. K. (2010): Hormones, nicotine, and cocaine: clinical studies. *Horm Behav.* **58**, 57–71
<https://doi.org/10.1016/j.yhbeh.2009.10.003>
- Padmavathi P., Reddy V. D., Kavitha G., Paramahamsa M., Varadacharyulu N. (2010): Chronic cigarette smoking alters erythrocyte membrane lipid composition and properties in male human volunteers. *Nitric Oxide* **23**, 181–186
<https://doi.org/10.1016/j.niox.2010.05.287>
- Pryor W. A., Stone K. (1993): Oxidants in cigarette smoke: radicals, hydrogen peroxide, peroxyxynitrate, and peroxyxynitrite. *Ann. NY Acad. Sci.* **686**, 12–28
<https://doi.org/10.1111/j.1749-6632.1993.tb39148.x>
- Reddy V. D., Padmavathi P., Paramahamsa M., Varadacharyulu N. C. (2009): Modulatory role of *Emblica officinalis* against alcohol induced biochemical and biophysical changes in rat erythrocyte membranes. *Food Chem. Toxicol.* **47**, 1958–1963
<https://doi.org/10.1016/j.fct.2009.05.014>
- Rose G. D., Glerasch L. M., Smith J. A. (1985): Turns in peptides and proteins. *Adv. Protein Chem.* **37**, 1–109
[https://doi.org/10.1016/S0065-3233\(08\)60063-7](https://doi.org/10.1016/S0065-3233(08)60063-7)
- Roesel M., Ruttig A., Schumacher C., Heinz C., Heiligenhaus A. (2011): Smoking complicates the course of noninfectious uveitis. *Graefes Arch. Clin. Exp. Ophthalmol.* **249**, 903–907
<https://doi.org/10.1007/s00417-010-1597-1>
- Satici A., Bitiren M., Ozardali I., Vural H., Kilic A., Guzey M. (2003): The effects of chronic smoking on the ocular surface and tear characteristics: a clinical, histological and biochemical study. *Acta Ophthalmol.* **81**, 583–587
<https://doi.org/10.1111/j.1395-3907.2003.00158.x>
- Schultz C. P., Wolf V., Lange R., Mertens E., Wecke J., Naumann D., Zähringer U. (1998): Evidence for a new type of outer membrane lipid in oral spirochete *Treponema denticola*. *J. Biol. Chem.* **273**, 15661–15666
<https://doi.org/10.1074/jbc.273.25.15661>
- Sherif S. M. (2010): The impact of elevated blood glycemic level of patients with type 2 diabetes mellitus on the erythrocyte membrane: FTIR study. *Cell Biochem. Biophys.* **58**, 45–51
<https://doi.org/10.1007/s12013-010-9092-1>
- Sprague R. S., Stephenson A. H., Bowles E. A., Stumpf M. S., Lonigro A. J. (2006): Reduced expression of G(i) in erythrocytes of humans with type 2 diabetes is associated with impairment of both cAMP generation and ATP release. *Diabetes* **55**, 3588–3593
<https://doi.org/10.2337/db06-0555>
- Susi H., Timasheff S. N., Stevens L. (1967): Infrared spectra and protein conformations in aqueous solutions. I. The amide I band in H₂O and D₂O solutions. *J. Biol. Chem.* **242**, 5460–5466

- Swapna I., Sathyaikumar K. V., Murthy C. R., Dutta-Gupta A., Senthilkumar B. (2006): Changes in cerebral membrane lipid composition and fluidity during thioacetamide-induced hepatic encephalopathy. *J. Neurochem.* **98**, 1899–1907
<https://doi.org/10.1111/j.1471-4159.2006.04028.x>
- Szalontai B., Kóta Z., Nonaka H., Murata N. (2003): Structural consequences of genetically engineered saturation of the fatty acids of phosphatidylglycerol in tobacco thylakoid membranes. An FTIR study. *Biochemistry* **42**, 4292–4299
<https://doi.org/10.1021/bi026894c>
- Thorne J. E., Daniel E., Jabs D. A., Kedhar S. R., Peters G. B., Dunn J. P. (2008): Smoking as a risk factor for cystoids macular edema complicating intermediate uveitis. *Am. J. Ophthalmol.* **145**, 841–846
<https://doi.org/10.1016/j.ajo.2007.12.032>
- Zagorski M. G., Barrow C. J. (1992): NMR studies of amyloid betapeptides: protein assignments, secondary structure, and mechanism of an alpha-helix-beta-sheet conversion for a homologous, 28-residue N-terminal fragment. *Biochemistry* **31**, 5621–5631
<https://doi.org/10.1021/bi00139a028>

Received: July 18, 2016

Final version accepted: September 23, 2016

First published online: May 4, 2017